Research Article

A Measure of Similarity Between Trajectories of Vessels

Le QI [1] and Zhongyi ZHENG [1,*]

[1]*Navigation College, Dalian Maritime University, Dalian 116026, China*

___

Abstract

The measurement of similarity between trajectories of vessels is one of the kernel problems that must be addressed to promote the development of maritime intelligent traffic system (ITS). In this study, a new model of trajectory similarity measurement was established to improve the data processing efficiency in dynamic application and to reflect actual sailing behaviors of vessels. In this model, a feature point detection algorithm was proposed to extract feature points, reduce data storage space and save computational resources. A new synthesized distance algorithm was also created to measure the similarity between trajectories by using the extracted feature points. An experiment was conducted to measure the similarity between the real trajectories of vessels. The growth of these trajectories required measurements to be conducted under different voyages. The results show that the similarity measurement between the vessel trajectories is efficient and correct. Comparison of the synthesized distance with the sailing behaviors of vessels proves that results are consistent with actual situations. The experiment results demonstrate the promising application of the proposed model in studying vessel traffic and in supplying reliable data for the development of maritime ITS.

Keywords: Trajectories of vessels, Similarity measurement, Feature point, Synthesized distance

___

1. Introduction

Trajectory, which is the route of the movement of an object, contains significant spatial information that is necessary in studying the behaviors of vessels. With the development of information techniques, a growing amount of vessel movement information can be monitored, and voluminous records of historical trajectories can be stored [1]. Several new and efficient methods have been proposed to utilize big data in promoting the development of maritime intelligent traffic systems (ITS) [2–4]. Notably, similarity measurement between the trajectories of vessels is a fundamental issue that needs to be solved in these methods [5–7]. The raw trajectories of vessels usually include many redundant points, outliers, and other elements [8–9]. When the volume of trajectory data is large, similarity measurement requires the feature points to be extracted from trajectories [10–13]. Moreover, to study the traffic characteristics of vessels, the similarity measurement result must be consistent with the actual motion of vessels [14–17]. The trajectory spatial distance describes the motion position information, and the trajectory shape shows the changes in the motion direction. Therefore, an efficient model is necessary to consider both factors to solve the aforementioned problem.

2. State of the Art

A trajectory can be mathematically expressed as a vector curve [18–23]. To detect feature points, one can use the characteristic point detection algorithms from the image compression and matching research fields. Several characteristic point detection algorithms have been proposed and widely used in computer vision [24–28], pattern recognition, intelligent identification [29], and retrieval [30]. Awrangjeb et al. [31] identified five main detection steps from these algorithms, namely, edge extraction and selection [32–34], smoothing [35–39], estimation, characteristic point detection, and coarse-to-fine characteristic point tracking. However, these algorithms cannot directly detect the feature points of trajectories because the calculated results must meet the requirements of the similarity measurement model that is proposed in this paper. Therefore, improvements are required.

Fu et al. [40] classified the algorithms for measuring vector curve similarity into two categories. First, global similarity measurement algorithms, such as Fourier descriptor algorithm [41], moment invariant algorithm [42], curvature scale space algorithm [43], shape context algorithm [44], curvature tree algorithm [45], normalized parametric polar transform algorithm [46], neural-network-based algorithm, and symbolic representation algorithm, can perform effectively in cases where the trajectories are complete. Second, part-to-part similarity measurement algorithms are applicable in cases where the trajectories have been transformed via rotation, translation, or scaling. These algorithms, which include Euclidean transform algorithms, similarity-invariant algorithms based on polyline approximation, energy function algorithm, and state-of-the-art algorithm [47], adopt the local curve features by identifying the corresponding sub-curves of the two curves. These algorithms can also be divided into 3D trajectory similarity measurement algorithm [48] and 2D trajectory similarity measurement algorithm depending on the objects under study.

However, the aforementioned methods do not simultaneously consider shape difference and spatial

___

distance, thereby preventing their measurement results from reflecting actual vessel sailing behaviors. However, some studies have synthesized these two factors. Trajectory data are generally enormous and dynamic in practical applications; thus, the static algorithm cannot solve such problems efficiently because a large amount of computational resources and huge storage space are required. Therefore, the feature-point detection algorithm was proposed to reduce the consumption of computational resources and storage space.

The rest of this paper is organized as follows. Section 3 describes the methodology of the similarity measurement model. Section 4 presents the experiments in which the performance of the model was tested, including their results, analysis, and discussion. Section 5 concludes the paper.

3. Methodology

The model includes two main steps. In the first step, the feature points are detected to denoise the trajectories of the raw vessels and extract the feature points. In the second step, the synthesized distance, shape difference, and spatial distance between trajectories are calculated. The similarity between trajectories is then determined by synthesizing the two calculated results.

The proposed model can significantly reduce the computing cost in dynamic applications by calculating only the increasing segment in each execution because the feature points and synthesized distance from the last execution are still valid.

3.1 Feature-point Detection
A trajectory comprises feature points and the lines that connect them. Feature points are not only very important parts of trajectories but are also vital factors in examining vessel sailing behaviors. By extracting feature points from a trajectory, the main feature information on the trajectory can be obtained and the data volume can be compressed.

The proposed feature-point detection algorithm utilizes the detection technology from the fields of image compression and matching. This algorithm removes the noise and local variation of a trajectory by filtering, smoothing, and judging the steering action via course alteration as well as by determining the corresponding feature point of each steering action. This algorithm is also relevant in dynamic applications because the extracted feature points can be reused when the trajectories are increased.

A in Fig. 1 denotes the raw trajectory of a vessel. To alter a course macroscopically, curve smoothing must be performed to remove the local variation and noise that result from equipment failures and environmental influences. The course changing of the vessel, $\Delta\theta_A$, can then be achieved. To reflect vessel sailing behaviors, $\Delta\theta_A$ must be partitioned into several segments, with each segment being a candidate for course changing. $\Delta\theta_A'$ denotes the sum of altered courses in each segment. A threshold of $\Delta\theta_A'$ must be defined to obtain the strong and significant feature points of trajectory A, as well as to remove the weak and insignificant segments from the candidates. $\Delta\theta_{threshold\_A}$, which represents the threshold, is obtained from empirical results or calculated via the interval estimation method as follows:

$$\Delta\theta_{threshold\_A} = mean(|\Delta\theta_A'|) + std(|\Delta\theta_A'|) \qquad (1)$$

where $mean(|\Delta\theta_A'|)$ denotes the mean of all elements in set $\Delta\theta_A'$ and $std(|\Delta\theta_A'|)$ denotes the standard deviation of all elements in set $\Delta\theta_A'$. Fig. 2 shows the curves of $\Delta\theta_A$, $\Delta\theta_A'$, and $\pm\Delta\theta_{threshold\_A}$. The vessel has altered its course five times, and the five points of trajectory A can be determined. Using the origin and destination points, all feature points of trajectory A are extracted as shown in Fig. 3.
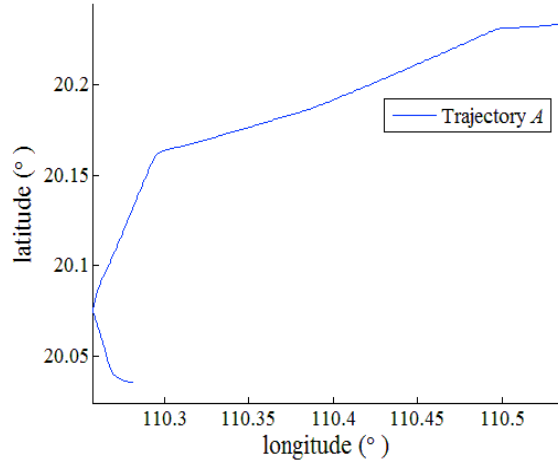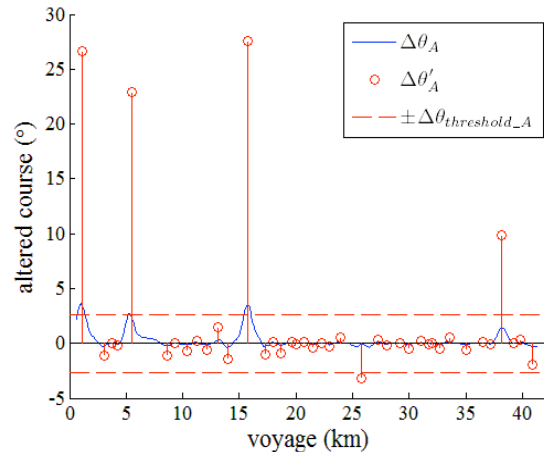

Fig. 1. Trajectory A.

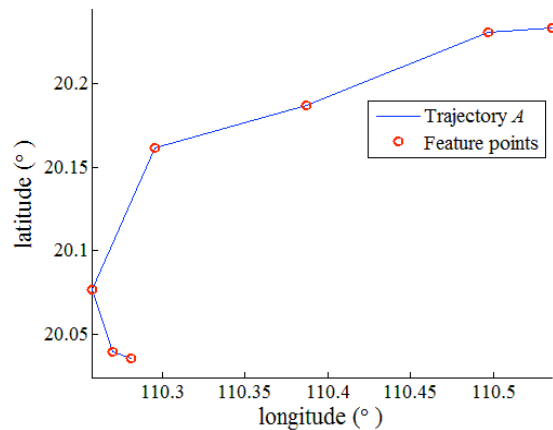**Fig. 2.** Curves of $\Delta\theta_A$, $\Delta\theta_A'$, and $\pm\Delta\theta_{threshold\_A}$.

Fig. 3. Feature points of trajectory A.
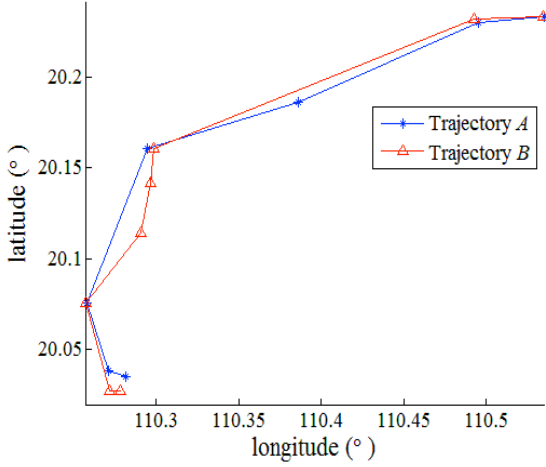
3.2 Synthesized Distance Calculation

Fig. 4. Trajectories *A* and *B*.

Fig. 5. Curves of Θ_A and Θ_B.

Fig. 5 shows the curves of $\Theta_A(f(s))$ and $\Theta_B(f(s))$.

First, the shape difference must be quantized. In Fig. 4, *B* denotes another trajectory that differs from trajectory *A*. Θ denotes the course when a vessel sails from one feature point to the next. (X_A, Y_A) denotes the feature points of trajectory *A* and can be computed as follows:

$$(X_A, Y_A) = \left\{ (X_A(i), Y_A(i)) \mid i = 0,1,\ldots,p+1 \right\}, \tag{2}$$

where *p*+1 denotes the number of feature points of trajectory *A*. The courses between the adjacent points in (X_A, Y_A) are computed as follows:

$$\Theta_A = \left\{ \Theta_A(i) \mid i = 0,1,\ldots,p \right\}, \tag{3}$$

where $\Theta_A(i)$ denotes the course from $(X_A(i), Y_A(i))$ to $(X_A(i+1), Y_A(i+1))$. (X_B, Y_B) denotes the feature points of trajectory *B* and can be computed as follows:

$$(X_B, Y_B) = \left\{ (X_B(i), Y_B(i)) \mid i = 0,1,\ldots,p'+1 \right\}, \tag{4}$$

where *p'*+1 denotes the number of feature points of trajectory *B*.

$$\Theta_B = \{ \Theta_B(i) \mid i = 0,1,\ldots,p' \}, \tag{5}$$

where $\Theta_B(i)$ denotes the course from $(X_B(i), Y_B(i))$ to $(X_B(i+1), Y_B(i+1))$.
Let

$$s_A = \left\{ s_A(i) \mid i = 0,1,\ldots,p+1 \right\}, \tag{6}$$

where $s_A(i)$ denotes the voyage from origin point $(X_A(0), Y_A(0))$ to $(X_A(i), Y_A(i))$. Let

$$s_B = \{ s_B(i) \mid i = 0,1,\ldots,p'+1 \}, \tag{7}$$

where $s_B(i)$ denotes the voyage from origin point $(X_B(0), Y_B(0))$ to point $(X_B(i), Y_B(i))$.

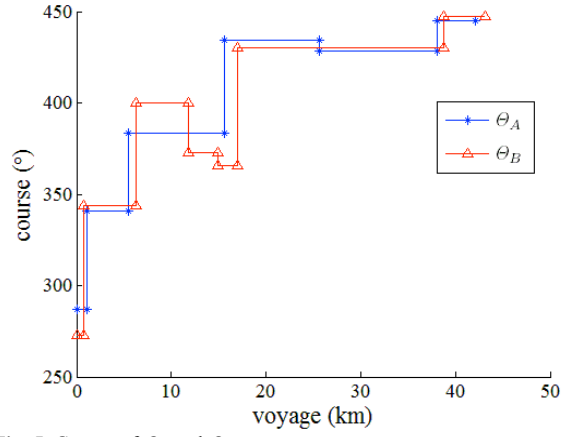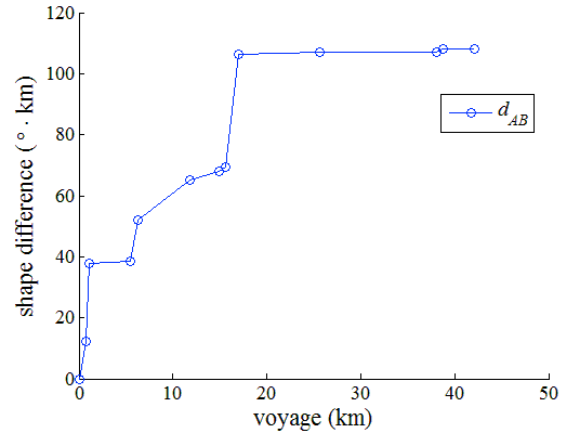$$i = f(s); if \ \ s(i) \leq s < s(i+1); i = 0,1,\ldots \tag{8}$$

Fig. 6. Shape difference between trajectories *A* and *B*.

Let *d* represent the shape difference between trajectories. The shape difference between trajectories *A* and *B* can be calculated as follows [23]:

$$d_{AB}(s) = \int_0^s \left| \Theta_A(f(s')) - \Theta_B'(f(s')) \right| ds'. \tag{9}$$

Fig. 6 shows the curve of $d_{AB}(s)$, which is not affected by the distance between the two trajectories. Thus, the translation movement of the trajectories does not affect the results of (9). The spatial distance between a couple of points of the two trajectories describes the translation distance.

Second, the distance between the representative points of trajectories *A* and *B* must be calculated. A couple of points must be chosen from trajectories *A* and *B*. The latest point of a trajectory is selected as the representative point because of its importance and easy calculation. Let *d'* denote the distance between representative points. Suppose that trajectories *B* and *A* are historical and new trajectories, respectively. The voyage of trajectory *A* is growing. The latest point of a trajectory *A* for a specific moment is $(X_A'(s), Y_A'(s))$, where *s* denotes the voyage from the origin point to $(X_A'(s), Y_A'(s))$. The total voyage of vessel *B* must not be shorter than *s* to calculate the distance. Thereafter, the point $(X_B'(s), Y_B'(s))$ of trajectory *B* must be obtained, and

the voyage from the origin point to this point is denoted by s. $(X_A'(s), Y_A'(s))$ and $(X_B'(s), Y_B'(s))$ are the representative points at the moment. The distance between the representative points of trajectories A and B is $d_{AB}'(s)$, which also denotes the spatial distance between trajectories A and B.

Third, the shape difference and spatial distance must be synthesized. Suppose that n voyages have been recorded during the growth of trajectory A, which is expressed as $\{S_i | i=1, 2, \ldots, n\}$. $S_i < S_{i+1}$, $i=1, 2, \ldots, n$. Therefore, the shape differences between trajectories A and B are expressed as follows:

$$\{d_{AB}(S_i) | i=1,2,\ldots,n\}. \tag{10}$$

The spatial distances between trajectories A and B are denoted as follows:

$$\{d_{AB}'(S_i) | i=1,2,\ldots,n\}. \tag{11}$$

Let D_{AB} denote the synthesized distances, which can be calculated as follows:

$$D_{AB}(S_i) = K_d \cdot \frac{d_{AB}(S_i)}{\text{Max}D} + (1-K_d)\frac{d_{AB}'(S_i)}{\text{Max}D'}; i=1,2, \quad ,n; 0 \leq K_d \leq 1, \tag{12}$$

where $\text{Max}D$ is the largest spatial distance, $\text{Max}D'$ is the largest shape difference, and K_d is the adjusting coefficient of shape difference and spatial distance. A larger K_d results in greater influence of shape difference on synthesized distance and smaller influence of spatial distance on synthesized distance. When $K_d = 1$, the synthesized distance describes the shape difference. When $K_d = 0$, the synthesized distance is the spatial distance. A smaller D_{AB} leads to greater similarities between trajectories A and B.

$$d_{AB}(S_{i+1}) = d_{AB}(S_i) + \int_{S_i}^{S_{i+1}} \left| \Theta_A(f(s')) - \Theta_B'(f(s')) \right| ds', i=1,2, \quad ,n-1. \tag{13}$$

Derived from (9) and (10), formula (13) indicates that if the last calculated result of shape difference is known, only the increased segment must be calculated to obtain the latest shape difference. The same characteristics are observed in calculating synthesized distance as shown in (12). Therefore, this algorithm can be used in dynamic applications.
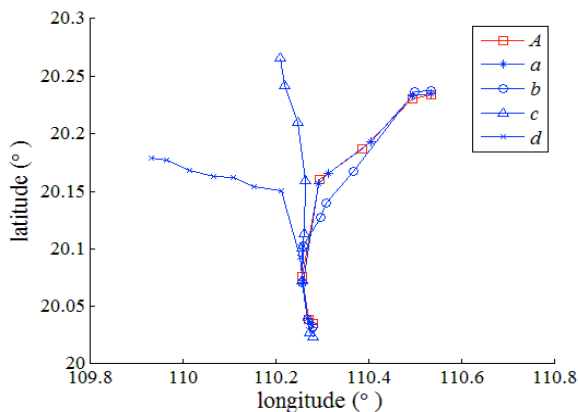
4. Analysis and Discussion

Fig. 7. Trajectories A, a, b, c, and d.

The data for trajectory A are collected from a vessel with a growing voyage. Four historical trajectories, namely, a, b, c, and d, are known. The similarities between A and the four trajectories must be measured following the aforementioned steps. The average data compression ratio of the five trajectories is 39.23. Fig. 7 shows the feature points of trajectories a, b, c, d, and A. a is the most similar trajectory to A, d is the most dissimilar trajectory to A, and b is more similar to trajectory A than to c.

$d_{Aa}(S)$, $d_{Ab}(S)$, $d_{Ac}(S)$, and $d_{Ad}(S)$ denote the shape differences of trajectory A from trajectories a, b, c, and d. S denotes the voyage. Fig. 8 shows that if $S \leq 15$ km, the shape difference between trajectories A and the four trajectories are resemblant. By contrast, if $S > 15$ km and S continues to grow, the shape difference between trajectories A and the four trajectories become inconsistent. The results in Fig. 8 are consistent with the shape features of trajectories in Fig. 7.

Let $d_{Aa}'(S)$, $d_{Ab}'(S)$, $d_{Ac}'(S)$, and $d_{Ad}'(S)$ denote the spatial distances of trajectory A from the other four trajectories. Fig. 9 shows that the spatial distances of A from c and d increase along with the growth of S. $d_{Ad}'(S)$ has a higher growth speed than $d_{Ac}'(S)$, but the spatial distances of A from a and b have not changed significantly. The results presented in Fig. 9 are also consistent with the features of trajectories shown in Fig. 7.
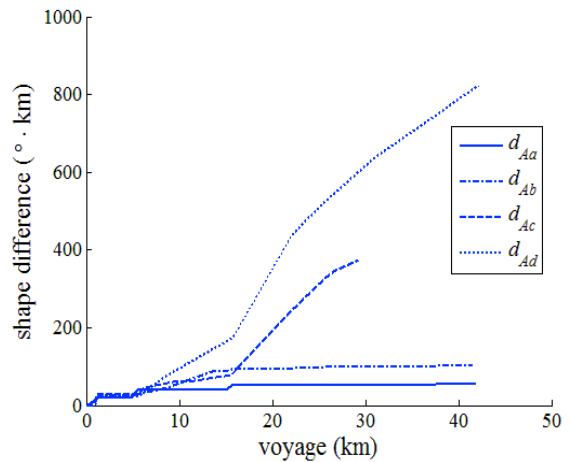

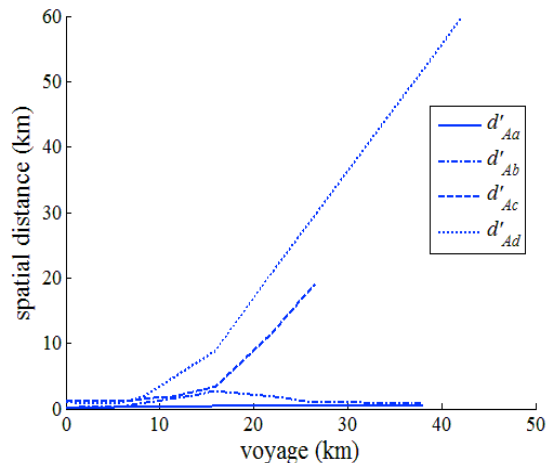**Fig. 8.** Shape differences between A and a, b, c, and d.

Fig. 9. Spatial distances of A from a, b, c, and d.

Table 1. Synthesized distances from trajectory A to trajectories a, b, c, and d.

S (km) / Trajectories	5	10	15	20	25	30	35	40
a	0.0144	0.0226	0.0217	0.0297	0.0297	0.0303	0.0306	--
b	0.0142	0.0396	0.0650	0.0657	0.0603	0.0589	0.0582	--
c	0.0225	0.0447	0.0637	0.1700	0.2955	--	--	--
d	0.0182	0.0756	0.1482	0.3177	0.4771	0.6110	0.7362	0.8581

When the shape difference and spatial distance are known, the synthesized distance can be calculated according to formula (12). Let Max$D$ = 60 km and MaxD' = 1000 °·km. Table 1 shows the calculated synthesized distance. When S = 5 km, d becomes the most similar trajectory to A. Trajectories a, c, and d are also very similar to trajectory A, but when $S \geq 10$ km, a becomes the most similar trajectory to A, while d remains the most dissimilar trajectory to A. The voyages of a, b, and c are shorter than 40 km; thus, some synthesized distances from A to these three trajectories cannot be calculated. The results in Table 1 are consistent with the features of trajectories in Fig. 7, which means that the similarity measurement results are consistent with the vessel sailing behaviors.

The similarities between the trajectories are measured by extracting the feature points and synthesizing shape difference and spatial distance. The data volume has been extremely compressed in the experiment. All feature points that are needed in the next step of the model have been retained. The proposed algorithm almost represents a lossless compression algorithm for measuring the similarity between trajectories because the course changing information is not deleted. Furthermore, the synthesized distances between a trajectory and the other four trajectories are calculated. The synthesized distance between the two most similar trajectories is 0.0306, and the highest dissimilarity of 0.7362 is obtained when the voyage is 35 km.

The calculations of the two abovementioned algorithms can be reused in dynamic applications. The proposed model is highly suitable for real-time applications, such as traffic detection and monitoring, because only the growth part of trajectories must be calculated when the voyages of vessels are increased.

Trajectory denotes the movement record of the vessel and is among the most important sources of data for vessel traffic research. The spatial distance between trajectories denotes the spatial distribution of traffic flow, whereas the shape differences between trajectories result from the different sailing behaviors of vessels. If the similarity between trajectories is measured by spatial distance, the individual differences in the maneuvering of vessels are ignored. By contrast, if such similarity is measured by shape difference, the location information of vessels is ignored.

Therefore, spatial distance and shape difference must be synthesized. The algorithm developed by Ping Xie is used to quantize shape difference [23]. The distance between the representative points of trajectories is calculated to measure the spatial distance between trajectories for two reasons. First, such distance can be easily calculated. Second, such distance emphasizes the latest distance between vessels in real-time application. This distance can also be replaced by another type of distance, such as the maximum distance and mean distance between trajectories, when needed.

Some attribute parameters, such as time, acceleration, and speed, are not considered in the model because they do not represent the information of a trajectory. The attribute information must be quantized according to professional knowledge and the specific application situation. The quantization results can be added to formula (12) in an appropriate form. Some parameters in the model, such as K_d, can be changed to extend the applicability of this model.

5. Conclusions

This paper proposed a model for measuring the similarity between the trajectories of vessels. The detection algorithm from the image compression and matching fields was imported and improved to extract feature points from raw trajectories. A new synthesized distance algorithm was then proposed to measure the similarity between trajectories. The experiment results show that the data have been compressed at a very high compression ratio. However, the important information, which is needed in the model, has been retained. By considering the shape difference and the spatial distance between trajectories, the synthesized distances successfully reflect the different motion behaviors of vessels and the disparity of the spatial distribution of trajectories. By reusing the measurement results, the similarity can be measured quickly and correctly when the trajectories are growing. The proposed algorithm can compress the data efficiently in real time to save storage space and computing resources. The measurement results have significant potential to support marine traffic research. Further research based on this model is necessary, especially for trajectory clustering, matching, and prediction.

References

1. Ray, C., Goralski, R., Claramunt, C., Gold, C., "Real-Time 3D Monitoring of Marine Navigation", *Information Fusion and Geographic Information Systems*, 2011, pp. 161-175.
2. Hadzagic, M., "Bayesian approaches to trajectory estimation in maritime surveillance", *McGill University*, 2010.
3. Perera, L. P., Soares, C. G., "Ocean Vessel Trajectory Estimation and Prediction Based on Extended Kalman Filter", *The Second International Conference on Adaptive and Self-Adaptive Systems and Applications*, 2010, pp. 14-20.
4. Perera, L. P., Oliveira, P., Soares, C. G., "Maritime Traffic Monitoring Based on Vessel Detection, Tracking, State Estimation, and Trajectory Prediction", *IEEE Transactions on Intelligent Transportation Systems*, 13(3), 2012, pp. 1188-1200.
5. Osborne, M., Pepper, J., "Creating Marine Spatial Data Infrastructure for the UK", *Coastal and Marine Geospatial Technologies*, 2010, pp. 51-55.
6. Pepper, J., "Unlocking the Marine Data Treasure Chest", *Coastal and Marine Geospatial Technologies*, 2010, pp. 57-64.

7. Wahyu, S., Pramono, G. H., Purnawan, B., "Establishment of Marine and Coastal Spatial Data Infrastructure in Indonesia", *Coastal and Marine Geospatial Technologies*, 2010, pp. 97-103.

8. Roh, G. P., Roh, J. W., Hwang, S. W., Yi, B. K., "Supporting Pattern-Matching Queries over Trajectories on Road Networks", *IEEE Transactions on Knowledge and Data Engineering*, 23(11), 2011, pp. 1753-1758.

9. Lin, L., Lu, Y., Pan, Y., Chen, X., "Integrating graph partitioning and matching for trajectory analysis in video surveillance", *IEEE transactions on Image Processing*, 21(12), 2012, pp. 4844-4857.

10. Hu, H., Zhou, J., "Trajectory Matching from Unsynchronized Videos", In: *IEEE Conference on Computer Vision and Pattern Recognition*, 2010, pp. 1347-1354.

11. Yang, D., Zhang, T., Li, J., Lian, X., "Synthetic Fuzzy Evaluation Method of Trajectory Similarity in Map-Matching", *Journal of Intelligent Transportation Systems*, 15(4), 2011, pp. 193-204.

12. Zdenek, K., Mikolajczyk, K., Matas, J., "Tracking-learning-detection", *IEEE Transactions on Pattern Analysis and Machine Intelligence*, 34(7), 2012, pp. 1409-1422.

13. Dodge, S., Laube, P., Weibel, R., "Movement similarity assessment using symbolic representation of trajectories", *International Journal of Geographical Information Science*, 26(9), 2012, pp. 1563-1588.

14. Buchin, M., Dodge, S., Speckmann, B., "Context-aware similarity of trajectories", *Geographic information science*, 2012, pp. 43-56.

15. Su, H., Zheng, K., Zeng, K., Huang, J., "Making sense of trajectory data: A partition-and-summarization approach", In: *IEEE 31st International Conference on Data Engineering*, 2015, pp. 963-974.

16. Gudmundsson, J., Laube, P., Wolle, T., "Computational movement analysis", *Springer Handbook of Geographic Information*, 2012, pp. 423-438.

17. Evans, M. R., Oliver, D., Shekhar, S., Harvey, F., "Summarizing trajectories into k-primary corridors: a summary of results", *Proceedings of the 20th International Conference on Advances in Geographic Information Systems*, 2012, pp. 454-457.

18. Zhang, X., Wang, H., Smith, A. W., Ling, X., Lovell, B. C., Yang, D., "Corner detection based on gradient correlation matrices of planar curves", *Pattern Recognition*, 43(4), 2010, pp. 1207-1223.

19. Awrangjeb, M., Lu, G., Fraser, C. S., "Performance comparisons of contour-based corner detectors", *IEEE Transactions on Image Processing*, 21(9), 2012, pp. 4167-4179.

20. Pinheiro, A. M. G., Ghanbari, M., "Piecewise Approximation of Contours Through Scale-Space Selection of Dominant Points", *IEEE Transactions on Image Processing*, 19(6), 2010, pp. 1442-1450.

21. Pedrosa, G. V., Barcelos, C. A. Z., "Anisotropic diffusion for effective shape corner point detection", *Pattern Recognition Letters*, 31(12), 2010, pp. 1658-1664.

22. Tabia, H., Daoudi, M., Vandeborre, J. P., Colot, O., "A New 3D-Matching Method of Nonrigid and Partially Similar Models Using Curve Analysis", *IEEE Transactions on Pattern Analysis and Machine Intelligence*, 33(4), 2011, pp. 852-858.

23. Xie, P., Ma, X., Zhang, X., Lin, M., "A New Fast Algorithm for Complex Polygons Matching", *Computer Engineering*, 29(16), 2003, pp. 177-178,181.

24. Aanæs, H., Dahl, A. L., Pedersen, K. S., "Interesting Interest Points", *International Journal of Computer Vision*, 97(1), 2012, pp. 18-35.

25. Rao, R. S., Ali, S. T., "A Computer Vision Technique to Detect Phishing Attacks", *2015 Fifth International Conference on Communication Systems and Network Technologies*, 2015, pp. 596-601.

26. Tian, Y., Yang, X., Yi, C., Arditi, A., "Toward a computer vision-based wayfinding aid for blind persons to access unfamiliar indoor environments", *Machine Vision and Applications*, 24(3), 2013, pp. 521-535.

27. Dandois, J. P., "Remote sensing of vegetation structure using computer vision", *University of Maryland*, 2014.

28. Solmaz, B., Assari, S. M., Shah, M., "Classifying web videos using a global video descriptor", *Machine Vision and Applications*, 24(7), 2013, pp. 1473-1485.

29. Xuan, Y., Coifman, B., "Identifying Lane-Change Maneuvers with Probe Vehicle Data and an Observed Asymmetry in Driver Accommodation", *Journal of Transportation Engineering*, 138(8), 2012, pp. 1051-1061.

30. Avila, S., Thome, N., Cord, M., Valle, E., Araujo, A. D. A., "Pooling in image representation: The visual codeword point of view", *Computer Vision and Image Understanding*, 117(5), 2013, pp.453-465.

31. Awrangjeb, M., Lu, G., Fraser, C. S., "Performance comparisons of contour-based corner detectors", *IEEE Transactions on Image Processing*, 21(9), 2012, pp. 4167-4179.

32. Kumar, K., Yadav, A., Rani, H., Nijhawan, Y., Radhika, S., "2-Dimensional Wavelet pre-processing to extract IC-Pin information for disarrangement analysis" *IOSR Journal of Electronics and Communication Engineering*, 7(6), 2013, pp. 36-38.

33. Chen, J., Takagi, N., "A Method to Extract Character Strings from Scene Images by Eliminating Non-character Strings: Towards Development of a Visual Assistance System for People with Visual Impairments" *2013 International Conference on Signal-Image Technology & Internet-Based Systems* , 2013, pp. 848-853.

34. Liu, F., Duan, H., Deng, Y., "A chaotic quantum-behaved particle swarm optimization based on lateral inhibition for image matching", *Optik-International Journal for Light and Electron Optics*, 123(21), 2012, pp.1955-1960.

35. Orzan, A., Bousseau, A., Barla, P., Winnemöller, H., Thollot, J., Salesin, D., "Diffusion curves: a vector representation for smooth-shaded images", *Communications of the ACM*, 56(7), 2013, pp. 101-108.

36. Mikulka, J., E Gescheidtova,., Bartusek, K., "Soft-tissues image processing: Comparison of traditional segmentation methods with 2D active contour methods", *Measurement Science Review*, 12(4), 2012, pp. 153-161.

37. Lawonn, K., Gasteiger, R., Rössl, C., Preim, B., "Adaptive and robust curve smoothing on surface meshes", *Computers & Graphics*, 40, 2014, pp. 22-35.

38. Yuen, A., Zhang, K., Altintas, Y., "Smooth trajectory generation for five-axis machine tools", *International Journal of Machine Tools and Manufacture*, 71, 2013, pp. 11-19.

39. Zhang, L., Gao, H., Chen, Z., Sun, Q., Zhang, X., "Multi-objective global optimal parafoil homing trajectory optimization via Gauss pseudospectral method", *Nonlinear Dynamics*, 72(1), 2013, pp. 1-8.

40. Fu, H., Tian, Z., Ran, M., Fan, M., "Novel affine-invariant curve descriptor for curve matching and occluded object recognition", *Computer Vision, IET*, 7(4), 2013, pp. 279-292.

41. Osowski, S., Nghia, D. D., "Fourier and wavelet descriptors for shape recognition using neural networks - a comparative study", *Pattern Recognition*, 35(9), 2002, pp. 1949-1957.

42. Zhao, D., Chen, J., "Affine curve moment invariants for shape recognition", *Pattern Recognition*, 30(6), 1997, pp. 895-901.

43. Mokhtarian, F., Abbasi, S., "Shape similarity retrieval under affine transforms", *Pattern Recognition*, 35(1), 2002, pp. 31-41.

44. Ling, H., Jacobs, D. W., "Shape classification using the inner-distance", *IEEE Transactions on Pattern Analysis and Machine Intelligence*, 29(2), 2007, pp. 286-299.

45. Alajlan, N., Kamel, M. S., Freeman, G. H., "Geometry-based image retrieval in binary image databases", *IEEE Transactions on Pattern Analysis and Machine Intelligence*, 30(6), 2008, pp. 1003-1013.

46. Frejlichowski, D., "Analysis of Four Polar Shape Descriptors Properties in an Exemplary Application", *Computer Vision and Graphics*, 2010, pp. 376-383.

47. Cui, M., Femiani, J., Hu, J., Wonka, P., Razdan, A., "Curve matching for open 2D curves", *Pattern Recognition Letters*, 30(1), 2009, pp. 1-10.

48. Tran, C., Trivedi, M. M., "3-D posture and gesture recognition for interactivity in smart spaces", *IEEE Transactions on Industrial Informatics*, 8(1), 2012, pp. 178-187.